Published in final edited form as:
J Chem Neuroanat. 2010 December ; 40(4): 301–309. doi:10.1016/j.jchemneu.2010.09.003.

Agonist-induced internalization of kappa-opioid receptors in noradrenergic neurons of the rat locus coeruleus

B. A. S. Reyes, **Charles Chavkin***, and **E. J. Van Bockstaele**
Department of Neurosurgery, Farber Institute for Neurosciences, Thomas Jefferson University, Philadelphia, PA 19107

* Department of Pharmacology, University of Washington, Seattle, WA 98195

Abstract

Kappa opioid receptors (κOR) are positioned to modulate pre- and post-synaptic responses of norepinephrine-containing neurons in the rat locus coeruleus (LC). The ability of an acute systemic injection of a long acting κOR agonist, U50,488, to induce trafficking of κOR was assessed in the LC using immunogold-silver detection in male Sprague-Dawley rats. U50,488 administration shifted immunogold-silver labeling indicative of κOR from primarily plasmalemmal sites to intracellular sites when compared to vehicle-treated subjects. This translocation from the plasma membrane to the cytoplasmic compartment was prevented by pre-treatment with the κOR antagonist, norbinaltorphimine (norBNI). To determine whether agonist stimulation could induce adaptations in the expression of the noradrenergic synthesizing enzyme, dopamine beta hydroxylase (DβH), and κOR expression, Western blot analysis was used to compare expression levels of DβH and κOR following U50,488 administration. Expression levels for DβH and κOR were significantly increased following U50,488 administration when compared to controls. These data indicate that a systemic injection of a κOR agonist stimulates internalization of κORs in noradrenergic neurons and can impact κOR and DβH expression levels in this stress-sensitive brain region.

Keywords

KOR; U50; 488; dopamine-beta hydroxylase; electron microscopy

1. Introduction

The dynorphin (DYN)-kappa opioid receptor (κOR) system has been implicated in stress-induced vulnerability to drug abuse. Stress, which promotes relapse and can facilitate place preference for drugs of abuse, increases prodynorphin gene expression in the limbic system (Shirayama et al., 2004). Genetic deletion of prodynorphin or pharmacological antagonism of κOR prevents stress-induced preference, implicating the DYN system in stress-induced facilitation of drug abuse (Shirayama et al., 2004). Additionally, norbinaltorphimine (norBNI), a κOR antagonist, prevents stress-elicited behaviors that are endpoints of

Corresponding Author: Beverly A. S. Reyes, D.V.M., Ph.D., Department of Neurosurgery, Farber Institute for Neurosciences, Thomas Jefferson University, 900 Walnut Street, Suite 400, Philadelphia, PA 19107, Voice: (215) 503-3323, FAX: (215) 503-9238, Beverly.Reyes@jefferson.edu.

depression such as immobility in the forced swim test and passive behavior in learned helplessness (Mague et al., 2003; McLaughlin et al., 2003a; Shirayama et al., 2004; Beardsley et al., 2005; Bruchas et al., 2007).

Recent anatomical and physiological studies have shown that κORs are positioned to pre-synaptically modulate diverse afferent signaling in the locus coeruleus (LC) (Kreibich et al., 2008; Reyes et al., 2009), a noradrenergic nucleus that is particularly sensitive to novel or unexpected stimuli and is regulated by stress (Rasmussen et al., 1986; Grant et al., 1988; Devauges and Sara, 1990; Sara et al., 1995). As the primary source of norepinephrine in the brain, the LC is involved in the regulation of arousal, attention and vigilance (Berridge and Waterhouse, 2003; Valentino and Van Bockstaele, 2005) and receives diverse inputs from sensory, autonomic and limbic regions (Van Bockstaele et al., 2010; Aston-Jones et al., 1991).

Our previous studies demonstrated that κOR-labeled axon terminals in the LC formed excitatory-type (e.g. asymmetric) synapses with tyrosine hydroxylase (TH) -labeled dendrites and that κOR and DYN are localized in common axonal profiles (Reyes et al., 2009). Furthermore, microinfusion of U50,488, a selective κOR agonist, into the LC attenuated discharge evoked by a variety of stimuli such as sciatic nerve stimulation, auditory inputs, withdrawal from opiates and hypotensive stress (Kreibich et al., 2008). To further define modulation of noradrenergic neurons by κOR ligands, we investigated whether a κOR agonist, U50,488, causes re-distribution of κOR from the plasma membrane to the intracellular compartment using immunoelectron microscopic analysis. We also examined whether agonist stimulation could induce adaptations in the expression of the noradrenergic synthesizing enzyme, dopamine-β-hydroxylase (DβH) as well as κOR expression in the LC. For this, we used western blot analysis to compare expressionlevels of DβH and κOR following U50,488 administration.

2. Materials and Methods

2.1 Animals

Fifty adult male Sprague Dawley rats (Harlan Laboratories, Indianapolis, IN, USA) housed three to a cage (20°C, 12-h light, 12-h dark cycle lights on 0700) were used in this study. Food and water were freely available. The rats weighed 190–227 g upon arrival and were housed in the animal facility for at least 7 days before experimentation. All procedures conformed to The Institutional Animal Care and Use Committee at Thomas Jefferson University according to the revised *Guide for the Care and Use of Laboratory Animals* (1996), The Health Research Extension Act (1985) and the PHS Policy on Humane Care and Use of Laboratory Animals (1986). All efforts were made to utilize only the minimum number of animals necessary to produce reliable scientific data, and experiments were designed to minimize any animal distress.

2.2 Specificity of antisera

Characterization of the κOR antibody used in the present study was conducted in our previous reports (Reyes et al., 2009) and others (Drake et al., 1996). κOR is an affinity-purified polyclonal antibody raised against the carboxyl terminal 15 amino acids of the cloned rat κOR (RDVGGMNKPV) and was generated in rabbit. κOR antibody is widely used in immunohistochemistry and its specificity has been characterized by multiple approaches. Antibody specificity was confirmed by Western blotting, enzyme-linked immunosorbent assays and κOR immunolabeling in Xenopus oocytes (Drake et al., 1996). Incubating serial sections in primary κOR antiserum preabsorbed with 10 μM antigenic peptide showed no immunoreactivity. Blots incubated with 1.5 μg/ml of affinity-purified

κOR antiserum preincubated with antigenic peptide did not show any bands. The κOR antibody specificity was also demonstrated by κOR immunoreactivity in the forebrain and pons (Drake et al., 2007; Drake et al., 1997; Drake et al., 1996) and spinal cord (Wang et al., 2009). We previously reported κOR specificity by using HEK293 cells transiently transfected with pcDNA3-FLAG-rat κOR and double labeled with the M2 monoclonal antibody against FLAG where a consistent identical staining was observed indicating that the antibody used recognizes κOR (Reyes et al., 2009; Wang et al., 2009).

The immunogen for mouse monoclonal antiserum was raised against denatured TH from rat pheochromocytoma, labels a single band at approximately 62kD corresponding to TH, and does not cross-react with dopamine-β-hydroxylase, dihydropterdine reductase, phenylethanolamine-N-methyltransferase, phenylalanine hydroxylase or tryptophan hydroxylase. The antibody has wide species cross-reactivity. The specificity of the TH antibody has been examined by preabsorption of the antibody with a high concentration of TH (Van Bockstaele and Pickel, 1993). Omission of the primary antibody abolished any detectable immunoreactivity (Reyes et al., 2007).

The monoclonal antibody against the DβH was raised against purified bovine DβH. The specificity of the DβH antibody has also been demonstrated previously in our laboratory (Oropeza et al., 2007).In addition, preabsorption with the respective antigen (Alpha Diagnostics, San Antonio, TX) resulted in an absence of immunolabeling in tissue sections from the frontal cortex.

2.3 Pharmacological treatment

U50,488 (Sigma-Aldrich Inc., St. Louis, MO, USA) was injected intraperitoneally (i.p.) at a dose of 5 mg/kg. This dose was chosen since we have previously reported that this dose attenuated the magnitude of LC phasic discharge evoked by a variety of stimuli (Kreibich et al., 2008).

2.3.1 Acute administration—Eight rats received a single injection of 5.0 mg/kg U50,488 dissolved in 0.9% saline to a concentration of 5.0 mg/ml (administered in a volume of 1.0 ml/kg). Ten rats received a single injection of the vehicle (0.9% saline) in a volume of 1.0 ml/kg. Seventeen rats received a single injection of norBNI (Sigma). The dose and the time selected for administration of norBNI was based on our previous study (Wang et al., 2009) as well as others (Wang et al., 2008). The antagonist effect of norBNI has a well characterized delayed onset and persists over long periods of time (Endoh et al., 1992). 10.0mg/kg norBNI was dissolved in 0.9% saline to a concentration of 10.0mg/ml (administered in a volume of 1.0 ml/kg). Sixteen hours post-norBNI injection, seven rats received a single injection of 5.0 mg/kg U50,488 in a volume of 1.0 ml/kg while 10 rats received a single injection of the vehicle (0.9% saline) in a volume of 1.0 ml/kg. Both U50,488 and vehicle injections were administered i.p. 30 min prior to perfusion.

2.4 Immunofluorescence

Five naïve rats were deeply anesthetized with sodium pentobarbital (80 mg/kg; Ovation Pharmaceuticals, Inc., Deerfield, IL, USA) and transcardially perfused through the ascending aorta with 500 ml of 4% formaldehyde in 0.1 M phosphate buffer (PB; pH 7.4). Brains were removed, blocked, postfixed in 4% formaldehyde overnight at 4°C and stored in 30% sucrose solution in 0.1 M PB containing sodium azide at 4°C for few days. The rat brain was frozen using Tissue Freezing Medium (Triangle Biomedical Science, Durham, NC, USA). Frozen 30 μm-thick sections were cut in the coronal plane using a freezing microtome (Micron HM550 cryostat; Richard-Allan Scientific, Kalamazoo, MI, USA) and collected in 0.1 M PB. Sections were placed for 30 min in 1% sodium borohydride in 0.1 M

PB to reduce amine-aldehyde compounds. The tissue sections were then incubated in 0.5% bovine serum albumin (BSA) and 0.25% Triton X-100 in 0.1 M tris-buffered saline (TBS; pH 7.6) for 30 min. Thorough rinses in 0.1 M TBS were done following incubation. Subsequently, sections were incubated in rabbit anti-κOR at 1:500 and mouse anti-TH (Immunostar Inc., Hudson, WI, USA) at 1:1,000 in 0.1% BSA and 0.25% Triton X-100 in 0.1M TBS. Incubation time was 15–18 hours in a rotary shaker at room temperature. Sections were then washed in 0.1 M TBS and incubated in a secondary antibody cocktail containing fluorescein isothiocyanate (FITC) donkey anti-rabbit (1:200; Jackson ImmunoResearch Laboratories Inc., West Grove, PA, USA) and tetramethyl rhodamine isothiocyanate (TRITC) donkey anti-mouse (1:200; Jackson ImmunoResearch) antibodies prepared in 0.1 % BSA and 0.25% Triton X-100 in 0.1 M TBS for 2 hours in the dark on a rotary shaker.

2.5 Immunoelectron microscopy

Rats acutely treated with vehicle with (n=3) or without (n=4) norBNI, and rats acutely treated with U50,488 with (n=3) or without (n=4) norBNI were anesthetized with sodium pentobarbital (60 mg/kg) 30 minutes following U50,488 injection, and perfused transcardially through the ascending aorta with 10 ml heparinized vehicle followed with 50 ml of 3.75% acrolein (Electron Microscopy Sciences, Fort Washington, PA, USA) and 200 ml of 2% formaldehyde in 0.1 M PB. The brains were removed immediately after perfusion fixation, sectioned into 1–3 mm coronal slices and postfixed in the same fixative overnight at 4ºC.

Alternate 40-μm-thick coronal sections through the rostrocaudal extent of the LC were processed for electron microscopic analysis of κOR or κOR and TH following the protocol described earlier for immunofluorescence except that Triton X-100 was not added to the solution for antibody incubation. Sections were incubated in rabbit anti-κOR at 1:500 or rabbit anti- κOR at 1:500 and mouse anti-TH (Immunostar Inc.) at 1:1,000 in 0.1% BSA in 0.1M TBS. Incubation time was 15–18 hours in a rotary shaker at room temperature. In singly-labeled sections, κOR immunoreactivity was detected using immunogold-silver labeling. In sets of sections that were dual-labeled for κOR and TH, immunoperoxidase labeling was used to identify TH immunoreactivity while immunogold-silver labeling was used to identify κOR immunoreactivity. Following primary antibody incubation, tissue sections were rinsed three times in 0.1 M TBS and incubated in biotinylated donkey anti-mouse (1:400; Vector Laboratories, Burlingame, CA) for 30 min followed by rinses in 0.1 M TBS. Subsequently, a 30-minute incubation of avidin-biotin complex (Vector Laboratories) followed. For all incubations and washes, sections were continuously agitated with a rotary shaker. TH was visualized by a 4-min reaction in 22 mg of 3,3′-diaminobenzidine (Sigma-Aldrich Inc.) and 10 μl of 30% hydrogen peroxide in 100 ml of 0.1 M TBS.

For gold-silver localization of κOR, sections were rinsed three times with 0.1 MTBS, followed by rinses with 0.1 M PB and 0.01 M phosphate buffered vehicle (PBS; pH 7.4). Sections were then incubated in a 0.2% gelatin-PBS and 0.8% BSA buffer for 10 min and followed by incubation in goat anti-rabbit IgG conjugate in 1 nm gold particles (Amersham Bioscience Corp., Piscataway, NJ, USA) at room temperature for 2 h. Sections were then rinsed in buffer containing the same concentration of gelatin and BSA as above. Following rinses with 0.01 M PBS, sections were then incubated in 2% glutaraldehyde (Electron Microscopy Sciences) in 0.01 M PBS for 10 min. This procedure was followed by washes in 0.01 M PBS and 0.2 M sodium citrate buffer (pH 7.4). A silver enhancement kit (Amersham Bioscience Corp.) was used for silver intensification of the gold particles. The optimal times for silver enhancement were determined by empirical observation for each experiment and ranged between 8 and 10 min. Following intensification, tissue sections were rinsed in 0.2 M

citrate buffer and 0.1 M PB, and incubated in 2% osmium tetroxide (Electron Microscopy Sciences) in 0.1 M PB for 1 h, washed in 0.1 M PB, dehydrated in an ascending series of ethanol followed by propylene oxide and flat embedded in Epon 812 (Electron Microscopy Sciences; Leranth and Pickel, 1989).

Thin sections of approximately 50–100 nm in thickness were cut with a diamond knife (Diatome-US, Fort Washington, PA, USA) using a Leica Ultracut (Leica Microsystems, Wetzlar, Germany). Captured images of selected sections were compared with captured light microscopic images of the block face before sectioning. Sections were collected on copper mesh grids, examined with an electron microscope (Morgagni, Fei Company, Hillsboro, OR, USA) and digital images were captured using the AMT advantage HR/HR-B CCD camera system (Advance Microscopy Techniques Corp., Danvers, MA, USA). Figures were assembled and adjusted for brightness and contrast in Adobe Photoshop.

2.6 Controls and data analysis

Some sections were processed in parallel with the rest of the procedures identical but one of the primary antisera was omitted. Sections processed in the absence of primary antibody did not exhibit immunoreactivity. To evaluate cross-reactivity of labeling of the primary antiserum by secondary antisera, some sections were processed for dual labeling with omission of one of the primary antisera. Tissue sections were taken from three to four rats per group with the good preservation of ultrastructural morphology and with clearly apparent immunocytochemical labeling. At least 10 grids containing 5 to 10 thin sections each were collected from at least two plastic-embedded sections of the LC from each animal. The quantification of κOR-immunolabeled profiles were carried out at the plastic-tissue interface to ensure that immunolabeling was detectable in all sections used for analysis (Chan et al., 1990). To determine whether levels of spurious silver grains could contribute to false positives, blood vessels and myelinated axons (structures that should not contain κOR immunolabeling) were counted in random ultrathin sections. Minimal spurious labeling was identified. Therefore, the criteria for considering a process as immunolabeled was defined by the presence of at least 2–3 silver grains in a cellular profile. Only tissue sections that were singly labeled for κOR were used for the electron microscopic analysis. The identification of cellular elements was based on the standard morphological criteria (Peters and Palay, 1996). The analysis of κOR internalization in various groups studied was quantified by calculating the ratio of cytoplasmic to total immunogold-silver particles for each singly immunolabeled axonal and dendritic profile in individual rats. As with previous studies from our group (Reyes et al., 2006; Reyes et al., 2008; Wang et al., 2009), care was taken to ensure that control and experimental groups contained similarly sized profiles. There was no statistical difference in the size of profiles analyzed in any group examined. The number of axonal and dendritic profiles per animal included in the analysis ranged from 128–147 and from 122–134, respectively.

2.7 Identification of gold-silver labeling in profiles

Using electron microscopy in all rats analyzed, immunogold-silver labeling for κOR was identified in axon terminals and dendrites, sometimes in unmyelinated axons in the LC. Selective immunogold-silver labeled profiles were identified by the presence, in single thin sections, of at least two immunogold-silver particles within a cellular compartment. Whenever possible, the more lightly labeled axonal labeling for κOR was confirmed by detection in at least two serial sections. The criterion of two gold particles as indicative of κOR labeling is conservative and may have led to an underestimation of the number of κOR-labeled profiles. Another factor that may have led to the underestimation of labeled profiles is the limitation of immunocytochemical methods to detect trace amounts of κOR. Moreover, unbiased stereological methods were not used for counting labeled profiles, and

the results of the numerical analysis can only be considered to be an estimate of the numbers of synapses and labeled profiles.

2.8 Protein extraction

An additional two sets of rats received either U50,488 or vehicle. Thirty minutes following a single injection of 5.0 mg/kg U50,488 or vehicle, rats were anesthetized with isoflurane (Webster Veterinary, Sterling, MA, USA; 0.5–1.0%, in air) and euthanized. Considering that the LC is a small nucleus in the anterodorsal part of the pontine tegmentum (Swanson, 1976; Foote et al., 1983), care was taken to excise the LC with as little tissue from neighboring structures as possible. To this end, coronal sections at a level of 9.16 mm to 10.52 mm posterior to bregma (Paxinos and Watson, 1986) were obtained using a rat brain mold. Subsequently, the cerebellum was retracted and a trephine was used to punch out the LC region. It is likely that some neighboring nuclei including the mesencephalic trigeminal nucleus may have been present in the micropunches (Paxinos and Watson, 1986). Brain tissue was rapidly removed from each animal on ice. Using a trephine, the LC brain region was microdissected from each animal. LC was homogenized with a pestle and extracted in radioimmunoprecipitation assay lysis buffer (Santa Cruz Biotechnology, Santa Cruz, CA, USA) on ice for 20 min. Lysates were cleared by centrifugation at 13,000 rpm for 12 min at 41°C. Supernatants or protein extracts were diluted with an equal volume of Novex 2® tris glycine sodium dodecyl sulfate sample buffer (Invitrogen, Carlsbad, CA, USA) containing dithiothreitol (Sigma-Aldrich Inc.). Protein concentrations of the undiluted supernatants were quantified using the bicinchoninic acid protein assay reagent (Pierce, Rockford, IL, USA).

2.9 Western blot analysis

Cell lysates containing equal amounts of protein were separated on 4–12% tris-glycine polyacrylamide gels and then electrophoretically transferred to Immobilon-P polyvinylidene fluoride membranes (Millipore, Bedford, MA, USA). Membranes were incubated in rabbit anti-κOR at 1:200 or mouse anti-DβH at 1:200, primary antibody overnight and then in alkaline phosphatase-conjugated secondary antibodies for 30 min to probe for the presence of proteins using a Western blotting detection system (Western Breeze Chemiluminescent Kit; Invitrogen). Following incubation in a chemiluminescent substrate (Western Breeze Chemiluminescent Kit), blots were exposed to X-OMAT AR film (Kodak, Rochester, NY, USA) for different lengths of time to optimize exposures. κOR or DβH was readily detected by immunoblotting in rat LC extracts. κOR immunoreactivity was visualized as a single band that migrates at approximately 58 kDA, while DβH migrates at approximately 75 kDA. Blots were incubated in stripping buffer (Restore Stripping Buffer, Pierce) to disrupt previous antibody-antigen interactions and then re-probed with β-actin (1:5,000, Sigma-Aldrich Inc.) with 1-hour incubation to ensure proper protein loading. The density of each band was quantified using Un-Scan-It blot analysis software (Silk Scientific Inc., Orem, Utah, USA). κOR or DβH was normalized to β-actin immunoreactivity on each respective blot. Western blot data was analyzed using Student's *t*-test (GraphPad Prism 4, GraphPad Software, Inc., San Diego, CA, USA)

3. Results

3.1 Immunocytochemical distribution of κOR in LC

Consistent with our previous report, κOR immunoreactivity was frequently localized in axon terminals as well as in dendrites and somata of LC neurons, albeit less frequently (Reyes et al., 2009). When present in somata or dendrites, κOR immunoreactivity was associated with catecholaminergic-containing profiles as evidenced by the presence of the synthesizing enzyme, TH (Figure 1). Within postsynaptic processes, κOR immunoreactivity was also

identified within dendrites that lacked TH immunoreactivity and are presumed to be inhibitory interneurons (Aston-Jones et al., 2004). Using dual immunofluorescence detection and confocal microscopy, κOR immunoreactivity exhibited a punctate pattern of labeling, as previously described (Reyes et al., 2009), which was observed throughout the rostrocaudal segment of the LC. Specifically, immunoreactivity for κOR appeared uniformly distributed within the core of the LC (Figure 1A) and in the peri-coerulear (peri-LC) area (not shown). Anatomically, the core of the LC is enriched with TH-immunoreactive perikarya (Shipley et al., 1996; Bajic et al., 2000) while the peri-LC contains a robust distribution of TH-labeled dendrites (Shipley et al., 1996; Van Bockstaele et al., 1996). The distribution of κOR immunoreactivity observed in the dual immunofluorescence studies is supported by the localization of κOR at the ultrastructural level. Using immunoelectron microscopy, κOR immunoreactivity was detected in axon terminals (Figure 1D–E) and in dendritic profiles (Figure 1F). Some axon terminals contacted unlabeled dendrites (Figure 1D) while many others targeted TH-labeled dendrites (Figure 1E). Consistent with the confocal fluorescence microscopy, κOR immunoreactivity is also associated with TH-labeled dendrites (Figure 1F).

Using immunogold-silver detection, κOR immunoreactivity was distributed along the plasma membranes as well as within the cytoplasm of pre-synaptic cellular profiles (Figure 2A–C) and postsynaptic profiles (Figure 3A–C) as previously described (Reyes et al., 2009).

3.2 Agonist-induced internalization of κOR in LC

Our present results show that an injection of U50,488 at a dose that attenuated the phasic discharge of LC evoked by auditory stimuli and significantly decreased tonic activity of LC neurons (Kreibich et al., 2008) resulted in significant κOR internalization which was both apparent in axon terminals (Figure 2B) and dendrites (Figure 3B). Table 1 presents the mean ratio of cytoplasmic to total immunogold-silver particles in κOR-immunoreactive axon terminals and dendrites in LC following vehicle or U50,488 administration with or without norBNI. The mean ratio of cytoplasmic to total immunogold-silver particles in axon terminals following U50,488 injection was 0.76 ± 0.02 which was significantly different ($P < 0.001$) from vehicle-treated subjects (0.31 ± 0.02). Following U50,488 injection, the mean ratio of cytoplasmic to total immunogold-silver particles in dendrites was 0.77 ± 0.04 which was significantly different ($P < 0.001$) from vehicle (0.40 ± 0.02) and other treated groups (0.38 ± 0.05 for axon terminals and 0.44 ± 0.03 for dendrites in U50,488 + norBNI-treated group while 0.32 ± 0.07 for axon terminals and 0.46 ± 0.05 for dendrites in vehicle + norBNI). Furthermore, Table 1 shows the total number of immunogold-silver particles localized to the intracellular compartment or the plasma membrane in either axon terminals or dendrites of all the experimental groups studied. In dendrites, κOR immunoreactivity was associated with endosome-like structures (Figure 3B). Figure 2A shows that in axon terminals, a comparable ratio of cytoplasmic to total immunogold-silver particles was observed when compared to vehicle-treated rats (0.40 ± 0.02) norBNI+U50,488 (0.38 ± 0.05) and norBNI+vehicle (0.32 ± 0.07). Thus, pretreatment with norBNI prior to U50,488 administration prevented the U50,488-induced internalization in axon terminals. Likewise, in dendrites of rats pre-treated with norBNI prior to U50,488 injection (0.44 ± 0.03) and rats that received norBNI and vehicle (0.46 ± 0.05) a comparable ratio of cytoplasmic to total immunogold-silver particles was also observed with the vehicle-treated rats (0.40 ± 0.02) (Figure 3A, 3C) indicating that pretreatment with norBNI prevented κOR internalization not only in axon terminals but in dendrites as well. Agonist-induced internalization of κOR following U50,488 treatment was also evident in dendritic profiles obtained from sections that were dual labeled for κOR and TH (Fig. 4B). Dual labeled dendrites for κOR and TH showed that following saline or norBNI prior to U50,488 treatment, κOR labeling was more frequently observed along the plasma membrane.

3.3 U50,488 alters expression levels of DβH and κOR in LC

The LC was microdissected bilaterally and the expression levels of DBH and κOR were assessed using Western blot analysis (Figure 5). Following U50,488 injection, DβH expression level was significantly increased ($P < 0.05$) compared to the vehicle-treated control. Likewise, U50,488-treated rats exhibited higher levels ($P < 0.05$) of κOR expression compared to vehicle-treated control. When pre-treated with the KOR antagonist, norBNI, κOR expression was not significantly different from control.

4. Discussion

In a cellular environment, the role of LC neurons is pivotal in the regulation of arousal and facilitation of adaptive behavioral responses (Aston-Jones et al., 1984; Berridge and Waterhouse, 2003; Valentino and Van Bockstaele, 2005). While the LC noradrenergic system sends widespread projections throughout the neuraxis, multiple afferents also converge on the LC which in turn influences neuronal activity. We have recently shown that DYN-κOR system modulates diverse afferent signaling to the LC (Kreibich et al., 2008; Reyes et al., 2008; Reyes et al., 2009). Thus, modulation of LC neuronal activity through the DYN-κOR system could be relevant to the cognitive and behavioral responses of noradrenergic neurons to stress.

The results of the present study provide evidence for κOR modulation of LC neuronal activity. Specifically, parenteral treatment of a κOR agonist, U50,488 results in the trafficking of the κOR in the LC. However, this trafficking was attenuated by a pre-administration of a κOR antagonist, norBNI. Concomitant with κOR trafficking is increases in the expression levels of DBH and κOR in the LC.

4.1 Technical considerations

In the present study, the specificity of the antisera was previously characterized (Van Bockstaele and Pickel, 1993; Drake et al., 1996; Reyes et al., 2007; Reyes et al., 2008; Reyes et al., 2009). Omission of the primary antibody abolished any detectable immunoreactivity for κOR or TH (Reyes et al., 2007; Reyes et al., 2008; Reyes et al., 2009). The preembedding method provides distinct subcellular localization of reaction product while preserving ultrastructural morphology (Leranth and Pickel, 1989). Furthermore, preembedding method is more suitable than postembedding method for determining regional localization and for localization of immunoreactivity at the extrasynaptic sites (Lujan et al., 1996). However, immunolabeling in thick sections prior to embedding poses a caveat that is unique to this approach which involves the optimal penetration of an antibody in thick tissue sections. In order to minimize penetration problems because of the relative thickness of the tissue sections, we collected tissue sections near the tissue-Epon interface where penetration of antibody is optimal to ensure that immunolabeling was clearly detectable in sections included in the analysis (Chan et al., 1990). In addition, profiles were sampled only when both markers were clearly present in the fields included in the analysis. Furthermore, experimental groups were processed in parallel; therefore, this limitation should not contribute to group differences. Moreover, for dual-labeled tissue sections sampling was only done when both markers (κOR+TH) were detectable in sections used for analysis (Leranth and Pickel, 1989). Using the present methodology, we are unable to determine whether κOR is recycled back to the plasma membrane or degraded following internalization. The use of lysosomal markers would be useful in this regard. Nevertheless, our immunoelectron microscopic technique allows important visualization of receptor localization associated with the plasma membrane or the cytoplasmic compartment (Van Bockstaele et al., 2001; Reyes et al., 2006; Reyes et al., 2008).

4.2 Subcellular localization of κOR in the LC

Consistent with our recent report (Reyes et al., 2009), the present study identified κOR localization predominantly in presynaptic sites indicating a greater preponderance in axon terminals. κOR immunoreactivity was also localized in axons. In some profiles, postsynaptic κOR localization was evident in dendrites and somata. The prominent localization of κOR in axon terminals is indicative of a presynaptic influence of κOR activation in the LC which has been reported in other brain regions including hippocampal formation (Drake et al., 1996), dentate gyrus (Drake et al., 1996), ventral rostral medulla (Drake et al., 1996), nucleus accumbens (Svingos et al., 1999), medial prefrontal cortex (Svingos and Colago, 2002) Physiological studies have shown that κOR mediates presynaptic inhibition in multiple brain regions including hippocampus (Simmons and Chavkin, 1996), nucleus ambiguus (Wang et al., 2004) and rostral ventral medulla (Ackley et al., 2001). Moreover, the study of Ford and colleagues has demonstrated that in the ventral tegmental area, modulation of κORs can suppress dopamine release via pre- and postsynaptic actions of κOR selective agonists (Ford et al., 2007). Furthermore, our physiological studies have shown that intracoerulear microinjection of U50,488 attenuated phasic discharge evoked by various stimuli (Kreibich et al., 2008). Taken together, κOR can impact activity of LC neurons through presynaptic modulation.

The existence of κOR on noradrenergic neurons is consistent with reports from others (Mansour et al., 1994), albeit using other approaches that include in situ hybridization and receptor autoradiographic techniques. The postsynaptic localization of κOR has been reported in other brain regions including hippocampus (Halasy et al.,2000), medial prefrontal cortex (Svingos and Colago, 2002), rostral ventromedial medulla (Drake et al., 2004) and spinal cord (Wang et al., 2009; Harris et al., 2004). It is likely that the postsynaptic action of κOR selective agonists could suppress norepinephrine release via modulation of LC neurons as reported for dopamine release in the ventral tegmental area (Ford et al., 2007).

4.3 Characteristics of κOR internalization

G-protein coupled receptors are the largest family of integral membrane receptors. Following stimulation with agonists, G-protein coupled receptors are internalized (Yu et al., 1993; Lefkowitz, 1998; Finch et al., 2009). Receptor internalization serves not only to turn off persistent receptor signaling but it also allows cells to regulate sensitivity to subsequent agonist exposure. It is usually followed by resensitization and receptor recycling to the plasma membrane (Ferguson, 2001). These coordinated events prevent excessive receptor stimulation or periods of prolonged inactivity. Previous *in vitro* studies have demonstrated a dose dependent agonist-induced internalization of κOR. Whereas 0.1 and 1.0 μM U50,488 did not induce internalization of κOR, stimulation at a higher dose of 10 μM induced a robust internalization of κOR using cultured HEK293 cells (McLaughlin et al., 2003b; Jordan et al., 2000). Internalization of κOR is also agonist specific as epitope-tagged κOR in HEK293 cells did not show internalization following acute treatment with 10 μM of the selective mu-opioid receptor agonist, etorphine (Chu et al., 1997). Incubation with the κOR-selective antagonist, norBNI, in HEK cells prevented κOR trafficking (McLaughlin et al., 2003b).The agonist-induced internalization of κOR required serine phosphorylation on the receptor (McLaughlin et al., 2003b). It is thought that agonist-induced κOR desensitization initiates receptor internalization (Law et al., 1982; Puttfarcken et al., 1988).

Engaging κORs using pharmacological tools (e.g. U50,488) affects LC neuronal activity (Kreibich et al., 2008; Tokuyama et al., 1998), norepinephrine release in regions targeted by LC (Laorden and Milanes, 2000; Werling et al., 1988) and impacts behavioral output (Redila and Chavkin, 2008; Shannon et al., 2007; Valdez et al., 2007). The present study

adds to this literature by showing that acute agonist administration causes internalization of κORs in the LC and is accompanied by increases in the expression levels of κOR and DβH. In humans, acute effects of the κOR agonist, MR 2033 have shown that subjects treated with a low dose experienced increased anxiety, racing thoughts, feelings of body distortion and discomfort (Pfeiffer et al., 1986). Conversely, subjects treated with a high dose experienced severe disturbances in the perception of time and space, visual hallucinations and symptoms of derealization, depersonalization and loss of self-control (Pfeiffer et al., 1986). Other κOR agonists including enadoline and Cl-977 caused subjects to experience visual distortions, depersonalization, sedation, confusion and abnormal thinking (Walsh et al., 2001; Reece et al., 1994). In rodents, κOR agonists administration including salvinorin A and U69593 cause an increase immobility in the forced swim test (Carlezon et al., 2006; Mague et al., 2003). These studies indicate that κOR agonists induce an adverse effect on behavior in both humans and rodents. It is tempting to speculate that the manifestation of these behavioral changes in humans and rodents is associated with the internalization of κOR and the concomitant alteration of κOR and DβH expression in the LC. However, further studies are needed to address these issues.

In response to changes in the activity of LC as well as in response to changes in brain levels of norepinephrine, expression levels of DβH are tightly regulated. When κORs are engaged via exposure to U50,488, an increase in DβH may reflect an increase in the activity of noradrenergic LC neurons. The LC, known for its widespread divergence of noradrenergic terminals to all levels of the neuroaxis (Foote et al., 1983) is activated in stress-related psychiatric disorders (Sullivan et al., 1999; Zhu et al., 1999). In the present study, the ability of norBNI to reverse the effect of U50,488 in κOR internalization suggests that the κOR antagonist can be a potential component of a therapeutic regimen to treat stress-related psychiatric disorders

In summary, using immunoelectron microscopy, our results demonstrate agonist-induced internalization of κORs in axon terminals and dendrites of the LC. The ability of a κOR antagonist to prevent κOR trafficking is a potential approach in the regulation of LC activity in the presence of stressors that involve dysregulation of the dynorphin system.

Research highlights

- U50,488 administration shifted immunogold-silver labeling indicative of κOR from primarily plasmalemmal sites to intracellular sites when compared to vehicle-treated subjects.
- The U50,488-induced κOR translocation from the plasma membrane to the cytoplasmic compartment was prevented by pre-treatment with the κOR antagonist, norbinaltorphimine.
- U50,488 administration significantly increased the expression levels for DβH and κOR when compared to controls.
- These data indicate that a systemic injection of a κOR agonist stimulates internalization of κORs in noradrenergic neurons and can impact κOR and DβH expression levels in this stress-sensitive brain region.

Acknowledgments

We thank Ms. Mulan Li and Dr. Yaping Qian for their expert technical assistance. This project was supported by the National Institutes of Health grant DA 09082.

References

Ackley MA, Hurley RW, Virnich DE, Hammond DL. A cellular mechanism for the antinociceptive effect of a kappa opioid receptor agonist. Pain 2001;91:377–388. [PubMed: 11275396]

Aston-Jones, G.; Foote, SL.; Bloom, FE. Anatomy and physiology of locus coeruleus neurons: functional implications. In: Ziegler, M.; Lake, CR., editors. Norepinephrine (Frontiers of Clinical Neuroscience). Williams and Wilkins; Baltimore: 1984. p. 92-116.

Aston-Jones G, Shipley MT, Chouvet G, Ennis M, Van Bockstaele EJ, Pieribone V, Shiekhattar R, Akaoka H, Drolet G, Astier B. Afferent regulation of locus coeruleus neurons: anatomy, physiology and pharmacology. Prog Brain Res 1991;88:47–75. [PubMed: 1687622]

Aston-Jones G, Zhu Y, Card JP. Numerous GABAergic afferents to locus ceruleus in the pericerulear dendritic zone: possible interneuronal pool. J Neurosci 2004;24:2313–2321. [PubMed: 14999082]

Bajic D, Proudfit HK, Van Bockstaele EJ. Periaqueductal gray neurons monosynaptically innervate extranuclear noradrenergic dendrites in the rat pericoerulear region. J Comp Neurol 2000;427:649–662. [PubMed: 11056470]

Beardsley PM, Howard JL, Shelton KL, Carroll FI. Differential effects of the novel kappa opioid receptor antagonist, JDTic, on reinstatement of cocaine-seeking induced by footshock stressors vs cocaine primes and its antidepressant-like effects in rats. Psychopharmacology (Berl) 2005;183:118–126. [PubMed: 16184376]

Berridge CW, Waterhouse BD. The locus coeruleus-noradrenergic system: modulation of behavioral state and state-dependent cognitive processes. Brain Res Brain Res Rev 2003;42:33–84. [PubMed: 12668290]

Bruchas MR, Land BB, Aita M, Xu M, Barot SK, Li S, Chavkin C. Stress-induced p38 mitogen-activated protein kinase activation mediates kappa-opioid-dependent dysphoria. J Neurosci 2007;27:11614–11623. [PubMed: 17959804]

Carlezon WA Jr, Beguin C, DiNieri JA, Baumann MH, Richards MR, Todtenkopf MS, Rothman RB, Ma Z, Lee DY, Cohen BM. Depressive-like effects of the kappa-opioid receptor agonist salvinorin A on behavior and neurochemistry in rats. J Pharmacol Exp Ther 2006;316:440–447. [PubMed: 16223871]

Chan J, Aoki C, Pickel VM. Optimization of differential immunogold-silver and peroxidase labeling with maintenance of ultrastructure in brain sections before plastic embedding. J Neurosci Methods 1990;33:113–127. [PubMed: 1977960]

Chu P, Murray S, Lissin D, von Zastrow M. Delta and kappa opioid receptors are differentially regulated by dynamin-dependent endocytosis when activated by the same alkaloid agonist. J Biol Chem 1997;272:27124–27130. [PubMed: 9341153]

Devauges V, Sara SJ. Activation of the noradrenergic system facilitates an attentional shift in the rat. Behav Brain Res 1990;39:19–28. [PubMed: 2167690]

Drake CT, Chavkin C, Milner TA. Kappa opioid receptor-like immunoreactivity is present in substance P-containing subcortical afferents in guinea pig dentate gyrus. Hippocampus 1997;7:36–47. [PubMed: 9138667]

Drake CT, De Oliveira AX, Harris JA, Connor DM, Winkler CW, Aicher SA. Kappa opioid receptors in the rostral ventromedial medulla of male and female rats. J Comp Neurol 2007;500:465–476. [PubMed: 17120286]

Drake CT, Patterson TA, Simmons ML, Chavkin C, Milner TA. Kappa opioid receptor-like immunoreactivity in guinea pig brain: ultrastructural localization in presynaptic terminals in hippocampal formation. J Comp Neurol 1996;370:377–395. [PubMed: 8799863]

Endoh T, Matsuura H, Tanaka C, Nagase H. Nor-binaltorphimine: a potent and selective kappa-opioid receptor antagonist with long-lasting activity in vivo. Arch Int Pharmacodyn Ther 1992;316:30–42. [PubMed: 1326932]

Ferguson SS. Evolving concepts in G protein-coupled receptor endocytosis: the role in receptor desensitization and signaling. Pharmacol Rev 2001;53:1–24. [PubMed: 11171937]

Finch AR, Caunt CJ, Armstrong SP, McArdle CA. Agonist-induced internalization and downregulation of gonadotropin-releasing hormone receptors. Am J Physiol Cell Physiol 2009;297:C591–600. [PubMed: 19587220]

Foote SL, Bloom FE, Aston-Jones G. Nucleus locus ceruleus: new evidence of anatomical and physiological specificity. Physiol Rev 1983;63:844–914. [PubMed: 6308694]

Ford CP, Beckstead MJ, Williams JT. Kappa opioid inhibition of somatodendritic dopamine inhibitory postsynaptic currents. J Neurophysiol 2007;97:883–891. [PubMed: 17122312]

Grant SJ, Aston-Jones G, Redmond DE Jr. Responses of primate locus coeruleus neurons to simple and complex sensory stimuli. Brain Res Bull 1988;21:401–410. [PubMed: 3145784]

Halasy K, Racz B, Maderspach K. Kappa opioid receptors are expressed by interneurons in the CA1 area of the rat hippocampus: a correlated light and electron microscopic immunocytochemical study. J Chem Neuroanatomy 2000;19:233–241.

Harris JA, Chang PC, Drake CT. Kappa opioid receptors in rat spinal cord: sex-linked distribution differences. Neuroscience 2004;124:879–890. [PubMed: 15026128]

Jordan BA, Cvejic S, Devi LA. Kappa opioid receptor endocytosis by dynorphin peptides. DNA Cell Biol 2000;19:19–27. [PubMed: 10668788]

Kasar M, Mengi M, Yildirim EA, Yurdakos E. Different effects of tianeptine pretreatment in rats exposed to acute stress and repeated severe stress. Methods Find Exp Clin Pharmacol 2009;31:157–163. [PubMed: 19536358]

Kreibich AS, Reyes BAS, Curtis AL, Ecke L, Chavkin C, Van Bockstaele EJ, Valentino RJ. Presynaptic inhibition of diverse afferents to the locus coeruleus by kappa opiate receptors: a novel mechanism for regulating the central norepinephrine system. J Neurosci 2008;28:6516–6525. [PubMed: 18562623]

Laorden ML, Milanes MV. Effects of U-50,488H and U-50,488H withdrawal on catecholaminergic neurons of the rat hypothalamus. Life Sci 2000;66:803–815. [PubMed: 10698355]

Law PY, Hom DS, Loh HH. Loss of opiate receptor activity in neuroblastoma X glioma NG108-15 hybrid cells after chronic opiate treatment. A multiple-step process. Mol Pharmacol 1982;22:1–4. [PubMed: 6126803]

Lefkowitz RJ. G protein-coupled receptors. III. New roles for receptor kinases and beta-arrestins in receptor signaling and desensitization. J Biol Chem 1998;273:18677–18680. [PubMed: 9668034]

Leranth, C.; Pickel, VM. Electron microscopic preembedding double-labeling methods. In: Heimer, L.; Zaborszky, L., editors. Neuroanatomical tracing methods. Vol. 2. Plenum Press; New York: 1989. p. 129-172.

Lujan R, Nusser Z, Roberts JD, Shigemoto R, Somogyi P. Perisynaptic location of metabotropic glutamate receptors mGluR1 and mGluR5 on dendrites and dendritic spines in the rat hippocampus. Eur J Neurosci 1996;8:1488–1500. [PubMed: 8758956]

Mague SD, Pliakas AM, Todtenkopf MS, Tomasiewicz HC, Zhang Y, Stevens WC Jr, Jones RM, Portoghese PS, Carlezon WA Jr. Antidepressant-like effects of kappa-opioid receptor antagonists in the forced swim test in rats. J Pharmacol Exp Ther 2003;305:323–330. [PubMed: 12649385]

Mansour A, Fox CA, Meng F, Akil H, Watson SJ. Kappa 1 receptor mRNA distribution in the rat CNS: comparison to kappa receptor binding and prodynorphin mRNA. Mol Cell Neurosci 1994;5:124–144. [PubMed: 8032682]

McLaughlin JP, Marton-Popovici M, Chavkin C. Kappa opioid receptor antagonism and prodynorphin gene disruption block stress-induced behavioral responses. J Neurosci 2003a;23:5674–5683. [PubMed: 12843270]

McLaughlin JP, Xu M, Mackie K, Chavkin C. Phosphorylation of a carboxyl-terminal serine within the kappa-opioid receptor produces desensitization and internalization. J Biol Chem 2003b; 278:34631–34640. [PubMed: 12815037]

Oropeza VC, Mackie K, Van Bockstaele EJ. Cannabinoid receptors are localized to noradrenergic axon terminals in the rat frontal cortex. Brain Res 2007;1127:36–44. [PubMed: 17113043]

Paxinos, G.; Watson, C. The rat brain in stereotaxic coordinates. Elsevier Academic Press; New York: 1986.

Peters A, Palay SL. The morphology of synapses. J Neurocytol 1996;25:687–700. [PubMed: 9023718]

Pfeiffer A, Brantl V, Herz A, Emrich HM. Psychotomimesis mediated by kappa opiate receptors. Science 1986;233:774–776. [PubMed: 3016896]

Puttfarcken PS, Werling LL, Cox BM. Effects of chronic morphine exposure on opioid inhibition of adenylyl cyclase in 7315c cell membranes: a useful model for the study of tolerance at mu opioid receptors. Mol Pharmacol 1988;33:520–527. [PubMed: 2835651]

Rasmussen K, Strecker RE, Jacobs BL. Single unit response of noradrenergic, serotonergic and dopaminergic neurons in freely moving cats to simple sensory stimuli. Brain Res 1986;369:336–340. [PubMed: 3697750]

Redila VA, Chavkin C. Stress-induced reinstatement of cocaine seeking is mediated by the kappa opioid system. Psychopharmacology (Berl) 2008;200:59–70. [PubMed: 18575850]

Reece PA, Sedman AJ, Rose S, Wright DS, Dawkins R, Rajagopalan R. Diuretic effects, pharmacokinetics, and safety of a new centrally acting kappa-opioid agonist (CI-977) in humans. J Clin Pharmacol 1994;34:1126–1132. [PubMed: 7876406]

Reyes BAS, Chavkin C, Van Bockstaele EJ. Subcellular targeting of kappa-opioid receptors in the rat nucleus locus coeruleus. J Comp Neurol 2009;512:419–431. [PubMed: 19009591]

Reyes BAS, Drolet G, Van Bockstaele EJ. Dynorphin and stress-related peptides in rat locus coeruleus: contribution of amygdalar efferents. J Comp Neurol 2008;508:663–675. [PubMed: 18381633]

Reyes BAS, Fox K, Valentino RJ, Van Bockstaele EJ. Agonist-induced internalization of corticotropin-releasing factor receptors in noradrenergic neurons of the rat locus coeruleus. Eur J Neurosci 2006;23:2991–2998. [PubMed: 16819988]

Reyes BAS, Johnson AD, Glaser JD, Commons KG, Van Bockstaele EJ. Dynorphin-containing axons directly innervate noradrenergic neurons in the rat nucleus locus coeruleus. Neuroscience 2007;145:1077–1086. [PubMed: 17289275]

Reyes BAS, Valentino RJ, Van Bockstaele EJ. Stress-induced intracellular trafficking of corticotropin-releasing factor receptors in rat locus coeruleus neurons. Endocrinology 2008;149:122–130. [PubMed: 17947354]

Sara SJ, Dyon-Laurent C, Herve A. Novelty seeking behavior in the rat is dependent upon the integrity of the noradrenergic system. Brain Res Cogn Brain Res 1995;2:181–187. [PubMed: 7580400]

Shannon HE, Eberle EL, Mitch CH, McKinzie DL, Statnick MA. Effects of kappa opioid receptor agonists on attention as assessed by a 5–choice serial reaction time task in rats. Neuropharmacology 2007;53:930–941. [PubMed: 17959202]

Shipley MT, Fu L, Ennis M, Liu WL, Aston-Jones G. Dendrites of locus coeruleus neurons extend preferentially into two pericoerulear zones. J Comp Neurol 1996;365:56–68. [PubMed: 8821441]

Shirayama Y, Ishida H, Iwata M, Hazama GI, Kawahara R, Duman RS. Stress increases dynorphin immunoreactivity in limbic brain regions and dynorphin antagonism produces antidepressant-like effects. J Neurochem 2004;90:1258–1268. [PubMed: 15312181]

Simmons ML, Chavkin C. k-Opioid receptor activation of a dendrotoxin-sensitive potassium channel mediates presynaptic inhibition of mossy fiber neurotransmitter release. Mol, Pharmacol 1996;50:80–85. [PubMed: 8700123]

Sullivan GM, Coplan JD, Kent JM, Gorman JM. The noradrenergic system in pathological anxiety: a focus on panic with relevance to generalized anxiety and phobias. Biol Psychiatry 1999;46:1205–1218. [PubMed: 10560026]

Svingos AL, Colago EE. Kappa-Opioid and NMDA glutamate receptors are differentially targeted within rat medial prefrontal cortex. Brain Res 2002;946:262–271. [PubMed: 12137930]

Svingos AL, Colago EE, Pickel VM. Cellular sites for dynorphin activation of kappa-opioid receptors in the rat nucleus accumbens shell. J Neurosci 1999;19:1804–1813. [PubMed: 10024364]

Swanson LW. The locus coeruleus: a cytoarchitectonic, Golgi and immunohistochemical study in the albino rat. Brain Res 1976;110:39–56. [PubMed: 776360]

Takeda H, Tsuji M, Matsumiya T. Changes in head-dipping behavior in the hole-board test reflect the anxiogenic and/or anxiolytic state in mice. Eur J Pharmacol 1998;350:21–29. [PubMed: 9683010]

Tokuyama S, Zhu H, Wakabayashi H, Feng YZ, Ho IK. The role of glutamate in the locus coeruleus during opioid withdrawal and effects of H-7, a protein kinase inhibitor, on the action of glutamate in rats. J Biomed Sci 1998;5:45–53. [PubMed: 9570513]

Valdez GR, Platt DM, Rowlett JK, Ruedi-Bettschen D, Spealman RD. Kappa agonist-induced reinstatement of cocaine seeking in squirrel monkeys: a role for opioid and stress-related mechanisms. J Pharmacol Exp Ther 2007;323:525–533. [PubMed: 17702903]

Valentino, RJ.; Van Bockstaele, EJ. Functional interactions between stress neuromediators and the locus-coeruleus noradrenaline system. In: Steckler, TKN.; Reul, JMHM., editors. Handbood of stress and the brain. Elsevier; Amsterdam: 2005. p. 465-486.

Van Bockstaele EJ, Colago EEO, Moriwaki A, Uhl GR. Mu-opioid receptor is located on the plasma membrane of dendrites that receive asymmetric synapses from axon terminals containing leucine-enkephalin in the rat nucleus locus coeruleus. J Comp Neurol 1996;376:65–74. [PubMed: 8946284]

Van Bockstaele EJ, Commons KG. Internalization of mu-opioid receptors produced by etorphine in the rat locus coeruleus. Neuroscience 2001;108:466–477.

Van Bockstaele EJ, Pickel VM. Ultrastructure of serotonin-immunoreactive terminals in the core and shell of the rat nucleus accumbens: cellular substrates for interactions with catecholamine afferents. J Comp Neurol 1993;334:603–617. [PubMed: 8408768]

Van Bockstaele EJ, Reyes BAS, Valentino RJ. The locus coeruleus: A key nucleus where stress and opioids intersect to mediate vulnerability to opiate abuse. Brain Res 2010;1314:162–174. [PubMed: 19765557]

Walsh SL, Strain EC, Abreu ME, Bigelow GE. Enadoline, a selective kappa opioid agonist: comparison with butorphanol and hydromorphone in humans. Psychopharmacology (Berl) 2001;157:151–162. [PubMed: 11594439]

Wang X, Dergacheva O, Griffioen KJ, Huang ZG, Evans C, Gold A, Bouairi E, Mendelowitz D. Action of kappa and delta opioid agonists on premotor cardiac vagal neurons in the nucleus ambiguus. Neuroscience 2004;129:235–241. [PubMed: 15489045]

Wang Y, Chen Y, Xu W, Lee DY, Ma Z, Rawls SM, Cowan A, Liu-Chen LY. 2-Methoxymethyl-salvinorin B is a potent kappa opioid receptor agonist with longer lasting action in vivo than salvinorin A. J Pharmacol Exp Ther 2008;324:1073–1083. [PubMed: 18089845]

Wang Y, Xu W, Huang P, Chavkin C, Van Bockstaele EJ, Liu-Chen LY. Effects of acute agonist treatment on subcellular distribution of kappa opioid receptor in rat spinal cord. J Neurosci Res 2009;87:1695–1702. [PubMed: 19130621]

Werling LL, McMahon PN, Cox BM. Selective tolerance at mu and kappa opioid receptors modulating norepinephrine release in guinea pig cortex. J Pharmacol Exp Ther 1988;247:1103–1106. [PubMed: 2849659]

Yu SS, Lefkowitz RJ, Hausdorff WP. Beta-adrenergic receptor sequestration. A potential mechanism of receptor resensitization. J Biol Chem 1993;268:337–341. [PubMed: 8380158]

Zhu MY, Klimek V, Dilley GE, Haycock JW, Stockmeier C, Overholser JC, Meltzer HY, Ordway GA. Elevated levels of tyrosine hydroxylase in the locus coeruleus in major depression. Biol Psychiatry 1999;46:1275–1286. [PubMed: 10560033]

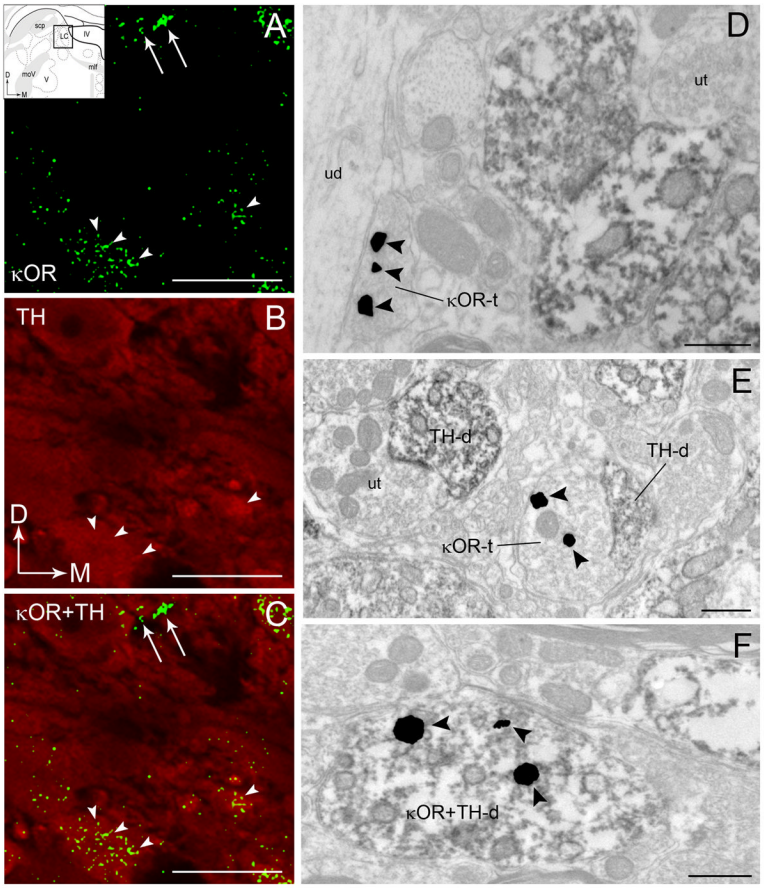

Figure 1.

A–C. Confocal fluorescence photomicrographs showing κOR and tyrosine hydroxylase (TH) immunoreactivities in the locus coeruleus (LC). κOR immunoreactivity was labeled with fluorescein isothiocyanate (green) and TH was labeled with rhodamine isothiocyanate (red). Arrowheads point to κOR-labeled processes that are localized in TH-labeled perikarya that can also be seen in the merged image in panel C. Arrows point to varicose processes that only contain κOR that are also seen in the merged image in panel C. Arrows indicate the dorsal (D) and medial (M) orientation of the tissue section. Inset shows schematic diagrams adapted from the rat brain atlas of Swanson (1992) depicting the LC region sampled. In the insets, arrows indicate dorsal (D) and medial (M) orientation of the sections illustrated. Abbreviations: scp, superior cerebellar peduncle; IV, fourth ventricle; mlf, medial longitudinal fasciculus; moV, motor root of the trigeminal nucleus; V, motor nucleus of the trigeminal nucleus. **D–F**. Electron photomicrographs showing immunoperoxidase labeling for TH and immunogold-silver labeling for κOR in the LC. **D.** An immunoperoxidase-labeled TH dendrite and an immunogold-silver labeled (arrowheads) κOR terminal (κOR-t) are seen in the same field. κOR-t targets an unlabeled dendrite (ud). Located nearby is an unlabeled axon terminal (ut) targeting a TH-d. **E.** An immunogold-silver labeled (arrowheads) κOR-t is shown contacting a TH-d. In the same field is shown an unlabeled terminal (ut) contacting a TH-d. **F.** A TH-d exhibiting immnoperoxidase labeling also exhibits immunogold-silver labeling (arrowheads) for κOR (κOR+TH-d). Scale bars, 100 μm (A-C), 0.5μm. (D–F).

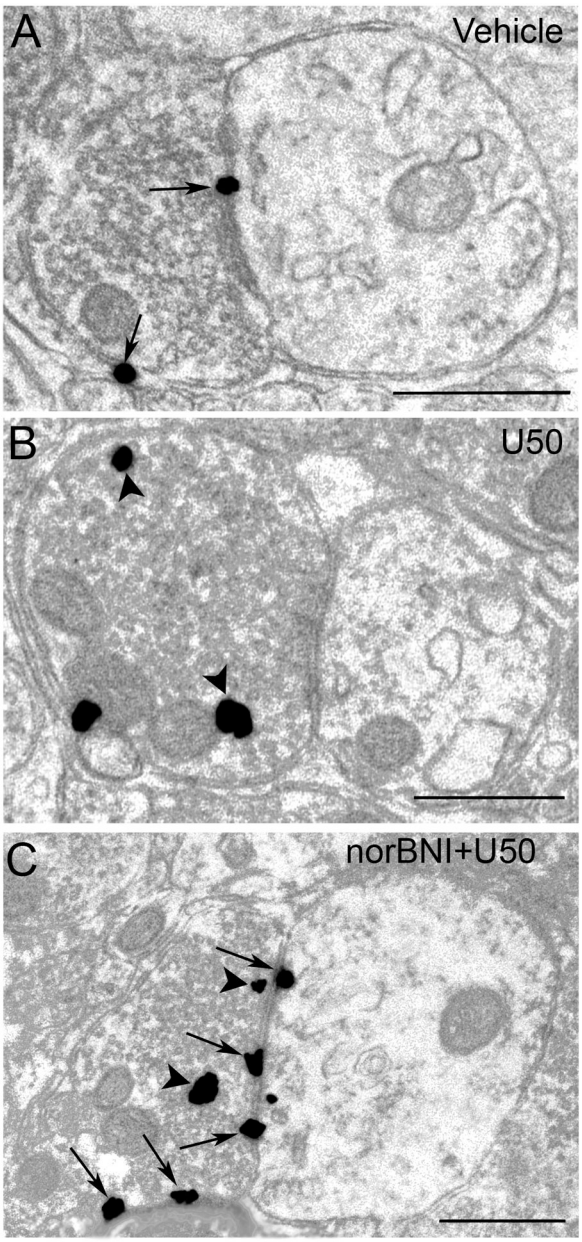

Figure 2.

Electron microscopic visualization evidence for U50488-induced internalization of κOR in locus coeruleus (LC) axon terminals. Sections from control (vehicle-treated) (A), U50488-treated (B) and norBNI-pretreated rats prior to U50488 treatment (C). **A.** Immunogold-silver labeling for κOR (arrows) can be seen along the plasmalemma in an axon terminal from vehicle-treated rats. **B.** κOR labeling shifts from the plasmalemma to the cytoplasm following U50488 in axon terminal. Arrowheads point to immunogold-silver labeling in the cytoplasm. **C.** Immunogold-silver labeling for κOR can be seen along the plasmalemma (arrows) and also in the cytoplasm (arrows) in an axon terminal from a norBNI-pretreated rat prior to U50488 treatment. Scale bars, 0.5μm.

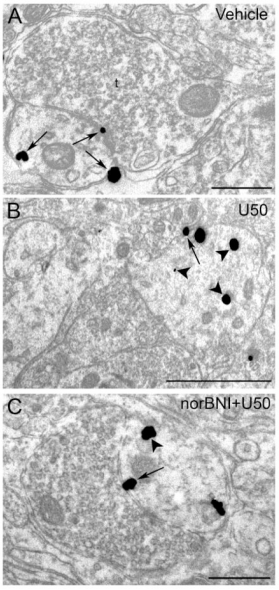

Figure 3.

Electron microscopic visualization evidence for U50,488-induced internalization of κOR in locus coeruleus (LC) dendrites. Sections from control (vehicle-treated) (A), U50,488-treated (B) and norBNI-pretreated rats prior to U50488 treatment (C). **A.** Immunogold-silver labeling for κOR (arrows) can be seen along the plasmalemma in a dendrite from vehicle-treated rats. A κOR-labeled dendrite receives synaptic contacts from an axon terminal (t). **B.** κOR labeling shifts from the plasmalemma (arrow) to the cytoplasm (arrowheads) in a dendrite following U50,488 treatment. Arrowheads point to immunogold-silver labeling in the cytoplasm. **C.** Immunogold-silver labeling for κOR can be seen along the plasmalemma (arrow) and also in the cytoplasm (arrowhead) in a dendritic profile following norBNI treatment prior to U50488 injection. Scale bars, 0.5μm.

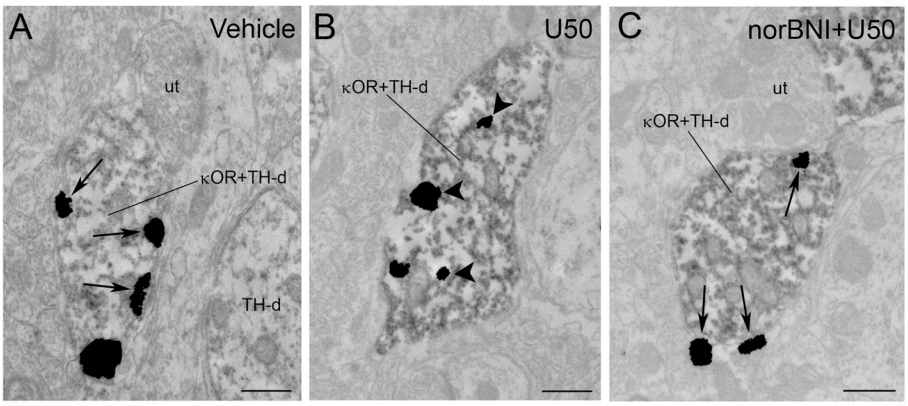

Figure 4.

Electron photomicrographs showing immunoperoxidase labeling for TH and immunogold-silver labeling for κOR in the locus coeruleus (LC) following vehicle (A), U50,488 (B) and norBNI-pretreated rats prior to U50488 treatment (C). **A.** A TH-labeled dendrite contains immunogold-silver labeling (arrows) for κOR distributed along the plasma membrane from a vehicle-treated control. The dually labeled dendrite (κOR+TH-d) is apposed to an unlabeled terminal (ut). A TH-labeled dendrite (TH-d) that does not contain κOR is found nearby. **B.** Shown is a TH-immunoperoxidase labeled dendrite containing immunogold-silver labeling for κOR (κOR+TH-d). κOR labeling shifts from the plasmalemma to the cytoplasm in a TH-labeled dendrite following U50,488 treatment. Arrowheads point to immunogold-silver labeling in the cytoplasm. **C.** Immunogold-silver labeling for κOR can be seen along the plasmalemma in a TH-labeled dendrite (κOR+TH-d) following norBNI treatment prior to U50,488 injection. Arrows point to κOR labeling along the plasma membrane. This κOR+TH-dual labeled dendrite is apposed by an unlabeled terminal (ut). Scale bars, 0.5μm.

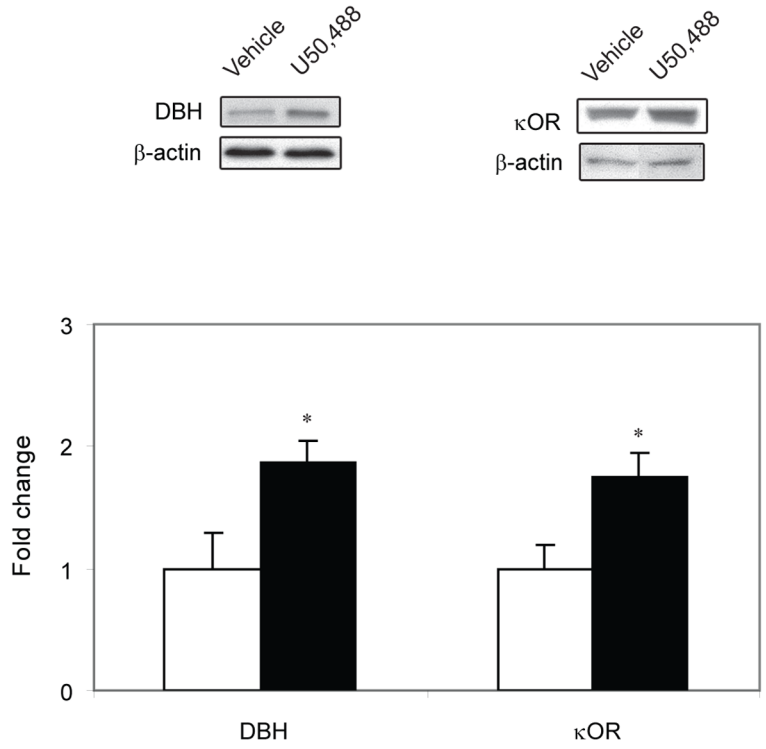

Figure 5.

Western blot analysis of dopamine beta hydroxylase (DβH) and kappa-opioid receptor (κOR) expression in the locus coeruleus following acute treatment of U50,488.κOR and DβH expression levels in the LC of the animals are expressed as a fold change from the control mean when the control equals 1.0 ± SEM. β-actin immunoblotting was used as a control to verify equal protein loading. DβH and κOR were significantly increased ($P < 0.05$) following U50,488 treatment compared to the control group. *$P < 0.05$ vs control group.Ms. Ref. No.: CHENEU-D-10-00031

Table 1

Ratio of cytoplasmic to total κOR-immunogold silver particles in the LC

	Axon terminals	Dendrites
Vehicle	0.31 ± 0.02	0.40 ± 0.02
U50,488	0.76 ± 0.02*	0.77 ± 0.04*
U50,488 + norBNI	0.38 ± 0.05	0.44 ± 0.03
Vehicle + norBNI	0.32 ± 0.07	0.46 ± 0.05

* $P < 0.001$ compared with all the vehicle and treatment groups

Number of κOR-immunogold-silver particles in axon terminals

	Total κOR- immunogold silver particles in PM	Total κOR- immunogold silver particles in IC	Total κOR- immunogold silver particles (PM+IC)
Vehicle	246.67 ± 15.88	115.33 ± 15.49	362.00 ± 31.26
U50,488	77.25 ± 13.52	240.75 ± 21.65	318.00 ± 34.81
U50,488 + norBNI	189.50 ± 29.65	124.25 ± 22.19	313.75 ± 25.93
Vehicle + norBNI	201.33 ± 10.60	100.00 ± 27.21	301.33 ± 24.36

Number of κOR-immunogold-silver particles in dendrites

	Total κOR- immunogold silver particles in PM	**Total κOR- immunogold silver particles in IC**	**Total κOR- immunogold silver particles (PM+IC)**
Vehicle	227.33 ± 10.69	164.67 ± 15.95	392.00 ± 23.52
U50,488	106.75 ± 20.16	355.50 ± 11.65	462.25 ± 27.67
U50,488 + norBNI	212.25 ± 35.25	188.00 ± 24.91	400.25 ± 49.14
Vehicle + norBNI	179.33 ± 3.71	168.00 ± 35.57	347.33 ± 39.28

Abbreviation: PM, plasma membrane; IC, intracellular compartment